Geochemistry Geophysics Geosystems G3

Article
Volume 13, Number 3
13 March 2012
Q03010, doi:10.1029/2011GC003910
ISSN: 1525-2027

Published by AGU and the Geochemical Society

The "van Zijl" Jurassic geomagnetic reversal revisited

Maud Moulin

Equipe de Paléomagnétisme, Institut de Physique du Globe, UMR 7154, Sorbonne Paris Cité, F-75005 Paris, France

Sciences de la Terre, de l'Environnement et des Planètes, Université Paris Diderot, Sorbonne Paris Cité, F-75013 Paris, France

Now at Département de Géologie, Université Jean Monnet, F-42023 Saint Etienne, France (maud.moulin@univ-st-etienne.fr)

Vincent Courtillot, Frédéric Fluteau, and Jean-Pierre Valet

Equipe de Paléomagnétisme, Institut de Physique du Globe, UMR 7154, Sorbonne Paris Cité, F-75005 Paris, France

Sciences de la Terre, de l'Environnement et des Planètes, Université Paris Diderot, Sorbonne Paris Cité, F-75013 Paris, France

[1] We have collected two new detailed records of what could be the second oldest well documented reversal, the "van Zijl" Jurassic (~180 Ma) reversal recorded in the thick basalt sequences of the Karoo large igneous province in Lesotho and South Africa. Sections yielded 10 and 8 independent transitional paleomagnetic directions respectively over two continuous 130 m and 160 m sequences. The corresponding VGP reversing paths share a number of consistent features and are integrated with a third record at Bushmen's Pass from Prévot et al. (2003) to yield a single reversal path with: 1- a large directional jump with no transitional poles between 45°S and 45°N in the first, main phase of the reversal, 2- a large elongated loop (multiple hairpin) to the SE with poles going down to ~20° latitudes in the second phase of the reversal, and 3- a rebound before finally settling in normal polarity. We have measured relative paleo-intensities on a set of carefully selected samples. Intensity was low prior to the directional changes and recovery to the following normal polarity was progressive. Transitional intensity is 80 to 90% lower than full polarity values. There is no significant increase in intensity at the time of transitional directional clusters. Our results are consistent with a weak non-dipolar reversing field, with faster and larger directional secular variation as the equator is crossed by VGPs. They tend to vindicate the notion of a short duration of the directional reversal, though one cannot draw global conclusions from a record limited to essentially a single location.

Components: 10,500 words, 10 figures, 2 tables.

Keywords: Jurassic; Karoo large igneous province; paleointensity; paleomagnetism; reversals.

Index Terms: 1521 Geomagnetism and Paleomagnetism: Paleointensity; 1535 Geomagnetism and Paleomagnetism: Reversals: process, timescale, magnetostratigraphy.

Received 26 October 2011; **Revised** 2 February 2012; **Accepted** 8 February 2012; **Published** 13 March 2012.

Moulin, M., V. Courtillot, F. Fluteau, and J.-P. Valet (2012), The "van Zijl" Jurassic geomagnetic reversal revisited, *Geochem. Geophys. Geosyst.*, *13*, Q03010, doi:10.1029/2011GC003910.

1. Introduction

[2] The evolution of the Earth's magnetic field is punctuated by occasional polarity reversals. The characteristics of the "transitional" field should provide important constraints for models of the geodynamo. The most direct evidence comes from the accumulation over the past four decades of paleomagnetic records obtained from sediments and volcanics. A major question has been to determine whether the transitional field had retained its dominant dipolar character during the reversal. To achieve this goal, paleomagnetists have used virtual geomagnetic poles (VGP). Publication of the first sufficiently detailed reversal records, with a large dispersion of VGPs as well as a large decrease of field intensity, made it obvious that these records were not compatible with a dipolar transitional field [*Dagley and Lawley*, 1974; *Hoffman*, 1977; *Fuller et al.*, 1979]. Subsequent observations have confirmed that VGP paths of the same reversal recorded in distinct locations were different [*Hillhouse and Cox*, 1976; *Valet et al.*, 1988; *Clement et al.*, 1982; *Valet et al.*, 1989] and that dipolar field intensity was reduced to at most 10% of its "full polarity" value [*Fuller et al.*, 1979; *Valet and Laj*, 1984; *Valet et al.*, 1988; *Chauvin et al.*, 1990; *Herrero-Bervera and Valet*, 2005; *Quidelleur and Valet*, 1996]. In addition, most detailed records display a complex pattern of directional changes that is reminiscent of the present non-axial dipole (NAD) field, i.e., with axial dipole removed [e.g., *Chauvin et al.*, 1989; *Mankinen et al.*, 1985; *Herrero-Bervera and Valet*, 1999; *Herrero-Bervera et al.*, 1999; *Brown et al.*, 2007; *Valet and Plenier*, 2008]. To our knowledge, no detailed study of a reversal has uncovered evidence of a strong transitional field.

[3] The database is divided in two distinct classes of records, from sediments and volcanics. It is not surprising that the two kinds of geological material provide different answers in the presence of a complex and rapidly changing field. The temporal continuity of slowly deposited sediments, significant advances in drilling marine cores and the development of highly sensitive magnetometers have favored the acquisition of a large number of sedimentary records of reversals. Records from sediments (with the exception of the last two reversals recorded in the northern Atlantic [*Channell and Lehman*, 1997]) cannot resolve features shorter than 1 ka (or even longer, if orientation of magnetic grains is only progressive). Statistical alignment of magnetic grains may not always reflect the orientation of magnetic field lines in the presence of the weak reversing field [*Valet et al.*, 1992; *Langereis et al.*, 1992]. For these reasons among others [see *Rochette*, 1990; *Langereis et al.*, 1992; *Quidelleur and Valet*, 1994; *Quidelleur et al.*, 1995; *Barton and McFadden*, 1996], we consider that whereas sediments are appropriate to document the evolution of the dipole field, they can rarely be used with confidence to extract information relevant to fast variations of the transitional field. Unresolved controversies over the past 20 years have been fueled by compilations of sedimentary records, suggesting that further progress should be expected from volcanic sequences.

[4] Indeed, magnetic directions from lava flows often provide more accurate, "snapshot-like" pictures of the reversing field, with the drawback that they generally form a discontinuous time sequence. Thus, knowledge of the exact stratigraphic succession of flows (in addition to radio-chronological dating) is essential to establish a detailed and accurate chronology. One must seek records derived from continuous, ordered sequences of flows; directions recorded from sparse or distant flows that cannot be unambiguously correlated and integrated within a succession of events are of limited use [*Valet and Herrero-Bervera*, 2003]. Unfortunately, not many studies satisfy these criteria. Their number is even more drastically reduced if one wants to rely only on records that document the evolution of the full paleomagnetic vector.

[5] An illustration of the direct consequence of incorporating too short sequences or scarce flows is given by compilations of volcanic records performed so far, which have yielded controversial conclusions, regarding for instance the existence of "preferential" longitudinal sequences of VGPs during the transitions. These bands had been first identified in sedimentary records, and their existence would have important consequences regarding the dynamo and geomagnetic features linked to structures in the lower mantle and core [*Laj et al.*, 1991; *Clement*, 1991]. A first compilation concluded that there was no evidence for such preferred bands [*Prévot and Camps*, 1993], whereas a subsequent analysis concluded in favor of a weak predominance of poles over the Americas and Asia [*Love*, 1998]. The two analyses relied on different assumptions and criteria for data selection. A more recent study [*Valet and Herrero-Bervera*, 2003], based on the most detailed volcanic records, has found "preferential bands" over not only the Americas and eastern Asia but also western Europe, failing to confirm the suggested links with lower

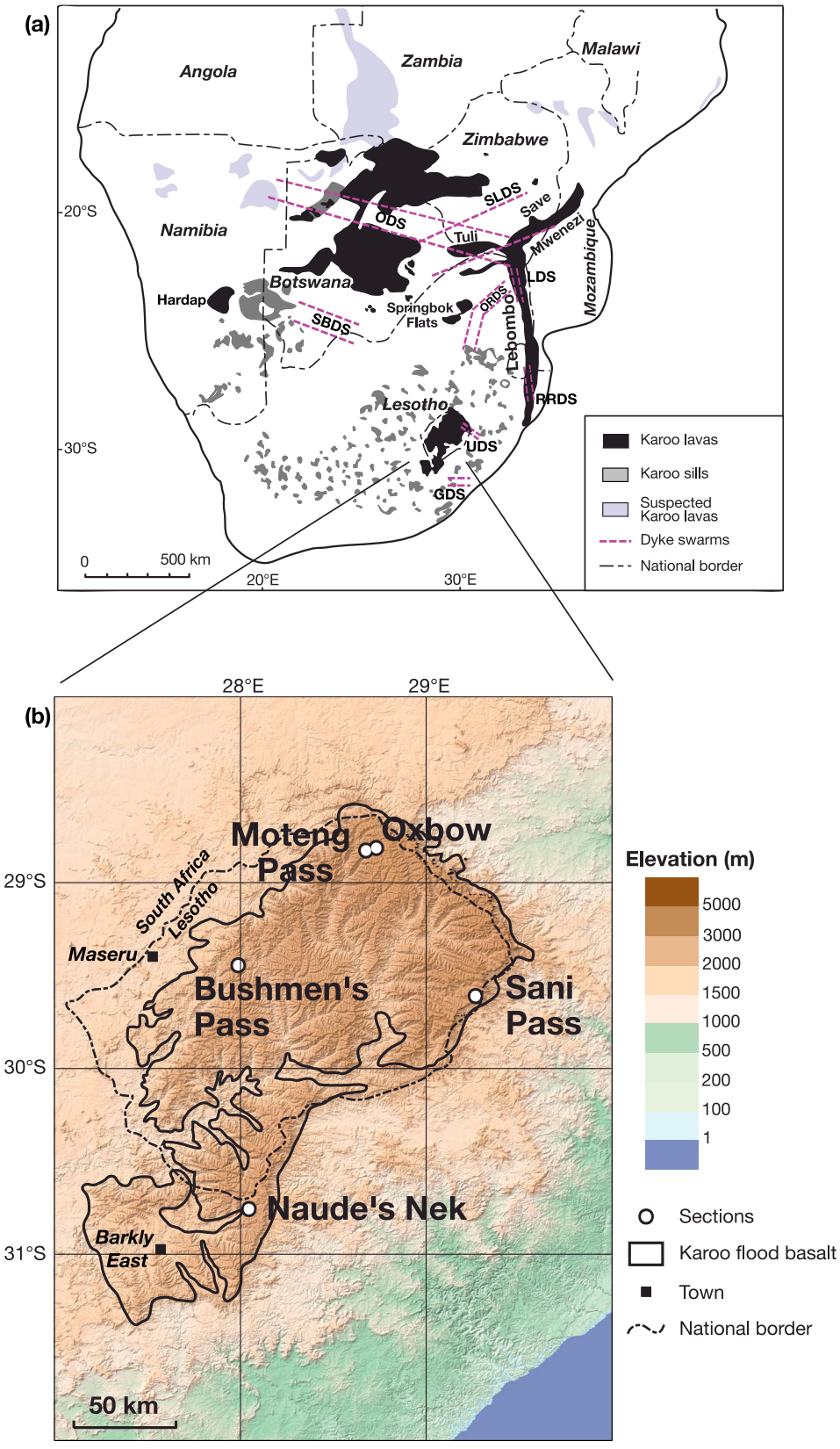

Figure 1. (a) Simplified geological map of southern Africa showing Karoo lavas (solid black: outcrops; pale blue: suspected), sills (gray) and dyke swarms (purple dashed lines) (modified after *Jourdan et al.* [2008]). (b) topography of the Lesotho part of the Karoo lavas with locations of the sections discussed in the paper.

mantle heterogeneities. However, in these studies, the number of records involved remained too small to allow a firm conclusion.

[6] Another characteristic feature of volcanic records is that VGPs often cluster around a few discrete locations and appear to jump from one such cluster to another remote location [e.g., *Prévot et al.*, 1985; *Hoffman*, 1992; *Riisager et al.*, 2002; *Valet and Herrero-Bervera*, 2003; *Heunemann et al.*, 2004]. For *Hoffman and Singer* [2008], clusters observed west of Australia and across Eurasia would correspond to persistent concentrations of the non-axial dipole field; VGPs calculated for the present non-dipole field are indeed in rather good coincidence with transitional paleomagnetic ones. However, these observations are derived from only a subset of volcanic records and the Australian patch appears to be controlled by the orientation of the equatorial dipole; this implies that a (non axial) dipole orientation would occasionally dominate during reversals and control field geometry, which is difficult to reconcile with our knowledge of the present field [*Valet and Plenier*, 2008; *Christensen et al.*, 2010]. Because the duration of a reversal is on the order of 10^4 years or less [*Clement*, 2004], geochronological methods (with typical uncertainties of ~1%) are unable to resolve time differences between VGPs within a reversal. The discontinuous nature of volcanic activity implies that the recorded reversal sequence is itself discontinuous and this has led to another debate: do the clusters reflect the fact that the dynamo may return to a fully dipolar yet non-axial state [*Hoffman*, 1992; *Coe et al.*, 2000] or do they simply reflect the episodic nature of volcanism [*Love*, 1998; *Valet and Herrero-Bervera*, 2003, 2011]?

[7] These ongoing debates about the detailed nature of geomagnetic reversals are not yet settled. Additional detailed volcanic data remain crucially needed to further advance these matters. Most of the above analyses rely on rather recent reversals, generally in the past 5 million years, notably the Brunhes-Matuyama reversal some 780,000 years ago. Pre-Neogene reversal records rely on volcanics. The three oldest obtained so far are a ~60 Myr reversal in the continental flood basalts of west Greenland [*Riisager et al.*, 2003], a Jurassic reversal discovered in the early sixties by *van Zijl et al.* [1962a, 1962b] in the Drakensberg formation of continental flood basalts in southern Africa (South Africa and Lesotho) and a ~250 Myr old reversal in the Siberian traps [*Heunemann et al.*, 2004].

[8] We have undertaken a comprehensive program (within the frame of the !Khure Africa joint South African - French research program) with the aim to describe completely the magnetic stratigraphy of the Drakensberg lavas over a total flow thickness exceeding 1600 m. We have relied on previous detailed petrological and chemical identification of lava formations [*Marsh and Eales*, 1984], and have undertaken geochronologic analyses using the non-conventional Cassignol-Gillot K-Ar and the more conventional $^{39}Ar/^{40}Ar$ techniques and extensive paleomagnetic analyses. One of the main aims of this program was to try to constrain the number of volcanic pulses and their individual and total durations and to analyze their potential links to the biotic (extinction) crises and environmental events that occurred near the Pliensbachian-Toarcian boundary. Full paleomagnetic and geochronological results are reported by *Moulin* [2011] and a summary of a part of the findings is given by *Moulin et al.* [2011]. Altogether, some 1670 paleomagnetic samples from 183 sites have been analyzed in three new sections: Naude's Nek, Moteng Pass and Oxbow (Figure 1). The present paper focuses on our re-sampling of and new results on what we propose to call the "van Zijl reversal."

2. Transitional Paleomagnetic Directions From the Naude's Nek and Moteng Pass Sections

[9] In their remarkable series of papers, *van Zijl et al.* [1962a, 1962b] provided evidence for the reversal, and analyzed the behavior of the field during the transition. This first detailed description of any geomagnetic reversal was based on some 150 samples from two sections at Bushmen's Pass and Sani Pass (Figure 1). The transitional directions were observed over some 150 m of section and described a zig-zag path going through about 10 points from reversed (below) to normal (above) polarity. Van Zijl et al. also attempted to determine the relative paleointensity of the field, comparing a thermal remanent magnetization (TRM) acquired in the laboratory to the natural remanent magnetization (NRM) of their field samples: they concluded that the field had decreased by a factor of 4 to 5 during the reversal. Although the methods used by van Zijl et al. are now considered superceded, one can only note how remarkably robust their main observations have remained. *Prévot et al.* [2003] returned to Bushmen's Pass and performed a more complete sampling of each flow over 340 m of

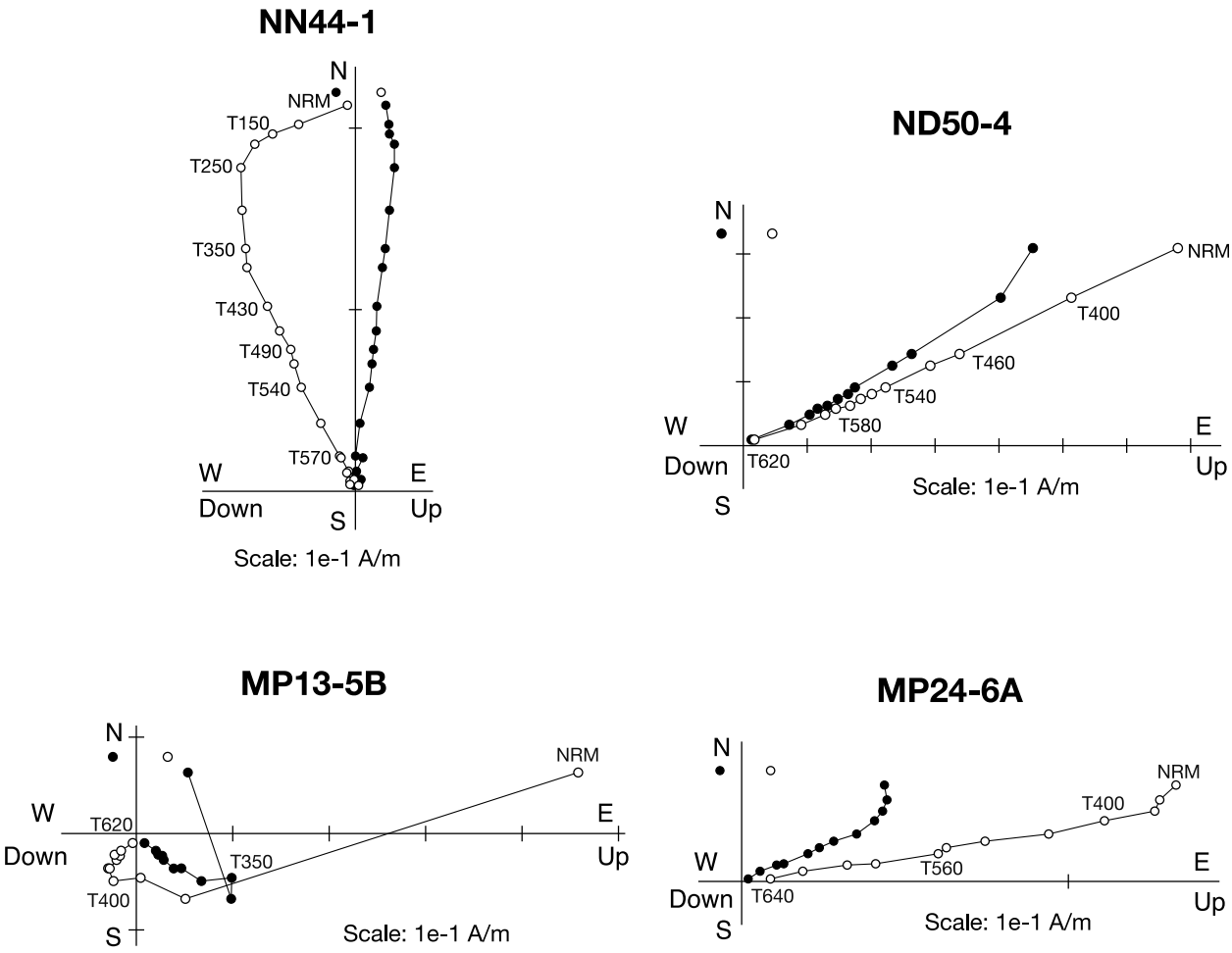

Figure 2. Four representative examples of vector demagnetization diagrams (thermal with temperature indicated) from transitional samples in the Naude's Nek (NN, ND) and Moteng Pass (MP) sections.

section, with 60 paleomagnetic sites and 4 to 8 samples per site when van Zijl et al. generally had a single sample. *Prévot et al.* [2003] found 35 transitional directions which amount to 21 distinct magnetic poles over 200 m of section. The VGP reversal path they obtained is more detailed and somewhat different from that of *van Zijl et al.* [1962a, 1962b] but they confirm that the field decreased by 80 to 90% in intensity during the reversal. We will return to their results in more detail in the discussion section of this paper. We next describe our new sections and the paleomagnetic results we have obtained.

2.1. Sections and Sampling

[10] The large Karoo flood basalt or large igneous province (LIP) is mainly composed of rather homogeneous tholeitic basalt flows erupted over a Triassic-Jurassic sedimentary basin (also called Karoo). The sections we have sampled come from the remnant of the Karoo LIP (Drakensberg group) that roughly corresponds to Lesotho but also outcrops in South Africa. We have sampled two sections at Naude's Nek in the South and a composite section in the North at Oxbow-Moteng Pass (Figure 1).

[11] The first flows in the Naude's Nek section overlie the Clarens formation, mainly composed of eolian sandstones that witnessed an arid climate. These flows belong to the Barkly East South Formation (Moshesh's Ford unit); they have reversed polarity and an age of 184.8 ± 2.6 Ma [*Moulin*, 2011; *Moulin et al.*, 2011]. This formation amounts to a rather small part (~10%) of the Drakensberg lavas. It is immediately covered by the main formation of the Drakensberg, the Lesotho Formation, in which a continuous section going from reversed to normal polarity has been sampled, and dated at ~179.2 ± 1.8 Ma [*Moulin*, 2011; *Moulin et al.*, 2011]. The reversal occurs near the

Table 1. Site Mean Magnetic Directions From Transitional Samples of the Naude's Nek and Oxbow Moteng Pass Sections[a]

Site	Directional Group or Single Flow	Elevation (m)	Slat (deg)	Slong (deg)	n/N	Dg (deg)	Ig (deg)	K	α_{95} (deg)
			Naude's Nek Section						
NN38	DG16	2060	−30.758	28.0591	8/8	4.2	6.4	792.3	2.1
NN39		2051	−30.758	28.0586	8/8	5.3	−11.6	28.4	10.8
NN40	DG16	2036	−30.759	28.0581	8/8	4.8	4.0	423.1	2.7
NN42	DG15	2020	−30.760	28.0577	8/8	−6.2	12.5	84.6	6.2
NN43		2015	−30.761	28.0574	5/8	−5.5	−22.5	42.2	11.9
NN44	DG15	2007	−30.762	28.0569	8/8	−3.8	19.8	53.2	7.8
NN45	DG15	2003	−30.763	28.0568	8/8	−1.5	21.4	187.4	4.1
NNPR	14	2002	−30.763	28.0554	9/9	24.1	−49.3	64.7	6.5
NN46	DG13	2001	−30.763	28.0555	8/8	55.8	−55.4	100.6	5.5
NN47	DG13	1993	−30.763	28.0562	7/8	60.2	−50.4	424.3	2.9
ND48		1992	−30.764	28.0561	7/7	52.8	−58.7	23.2	12.9
ND49	12	1990	−30.763	28.0519	8/8	39.5	−56.1	54.6	7.9
ND50		1986	−30.763	28.0489	4/5	52.2	−50.6	48.6	13.3
ND51	DG11	1973	−30.760	28.0444	8/8	6.8	−8.5	150.7	4.6
ND52	DG11	1967	−30.758	28.0416	8/8	4.7	−12.8	37.7	9.7
ND53	DG11	1957	−30.754	28.0339	8/8	−3.5	−16.7	52	8.3
ND54	10	1951	−30.753	28.0336	7/8	−9.7	−44.7	54.4	8.8
ND55	DG9	1950	−30.752	28.0334	8/8	3.5	−13.5	150.9	4.7
ND56	DG9	1946	−30.752	28.0297	7/8	−1.2	−11.9	122.3	6.0
ND57	8	1946	−30.752	28.0288	8/8	−2.9	−29.7	90.5	6.4
ND58	DG7	1938	−30.751	28.0266	8/8	−0.5	−19.5	34.1	9.9
ND59		1927	−30.754	28.0243	6/6	16.3	−23.3	44.1	11.4
ND60	DG7	1927	−30.753	28.0208	6/6	−2.4	−18.8	295.6	4.4
			Oxbow-Moteng Pass Section						
MP24	OM11	2247	−28.764	28.5767	8/8	68.2	−68.3	189.5	4.0
MP23	OM10	2226	−28.765	28.5749	7/8	86.2	−70.9	274.2	3.7
MP22	OM9	2212	−28.765	28.5741	8/8	64.3	−69	612.7	2.2
MP21	DG-OM8	2197	−28.765	28.5727	8/8	94.9	−72.8	234.3	3.6
MP20	DG-OM8	2174	−28.765	28.5700	6/8	97.9	−76.6	83.3	7.4
MP19	OM7	2158	−28.766	28.5694	7/8	38.8	−63.1	104	5.9
MP18	OM6	2150	−28.766	28.5687	6/8	6.4	−40.0	89.4	7.1
MP17	DG-OM5	2143	−28.766	28.5677	6/7	114.7	17.2	77.4	7.8
MP16	DG-OM5	2141	−28.766	28.5668	8/8	121.5	19.2	88.6	5.9
MP15	DG-OM5	2140	−28.765	28.5659	8/8	116.1	25	50.3	8.2
MP14		2121	−28.764	28.5617	7/8	138.4	18.4	32.3	10.9
MP13	OM4	2096	−28.762	28.5534	7/8	135.7	23.2	198.3	4.3

[a]Site mean magnetic directions are numbered from 7 to 16 for the Naude's Nek section (DGx when the site belongs to a directional group or x for a single flow) and 4 to 11 for the Oxbow-Moteng Pass section (DG-OMx when the site belongs to a directional group or OMx for a single flow) (see Table 2). Latitude Slat (deg) and longitude Slon (deg) are the coordinates of paleomagnetic sites; n/N, N is the number of samples measured, and n is the number used in calculating the mean direction; Dg and Ig are the site mean declination and inclination of the Characteristic Remanent Magnetization (ChRM); K is the Fisher precision parameter; α_{95} is the 95% confidence interval.

base, in the Mafika Lisiu unit. Lava flows from the Moshesh's Ford unit are significantly older than the upper part of the section and are therefore not further considered in the present paper.

[12] The base of the Moteng Pass section is more difficult to identify, as it corresponds to a level, widely cultivated area at the base of the main mountain section. But K-Ar and Ar-Ar dating seem to show that the lowermost flows, which have reversed polarity, have an age that cannot be distinguished from the lava pile above and are already in the Lesotho formation. Therefore, all data from the Oxbow-Moteng Pass section are retained in this paper. The reversal occurs near the base of the section on the well-exposed road going uphill into the Mafika Lisiu unit.

2.2. Paleomagnetic Analyses

[13] All paleomagnetic results on the reversed and normal series are given by *Moulin* [2011] and *Moulin et al.* [2011] (for the Naude's Nek section). The existence of well-defined successions of reversed and normal flows with opposite directions that can be correlated across several sections

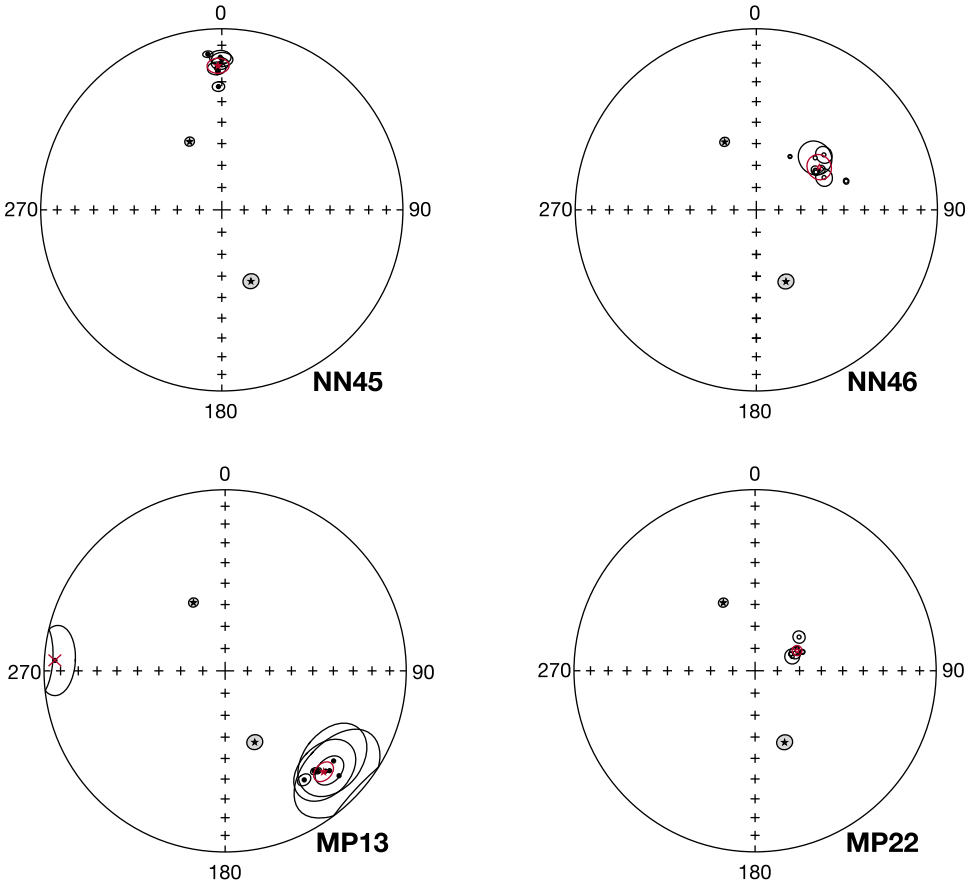

Figure 3. Four representative examples of stereographic sample directions and site means from transitional samples in the Naude's Nek (NN) and Moteng Pass (MP) sections. Means are in red, 95% confidence intervals are shown and the normal and reversed field during the chrons above and below the transition are shown as stars. An outlier which is not considered in calculating the site mean is shown as a red cross in site MP13.

strongly pleads in favor of the primary character of the magnetization. In this paper, we focus on the study of the transitional directions. We selected one specimen from each site for detailed thermal demagnetization with 12 to 19 successive steps, depending on the magnetic mineralogy of the samples. Alternating field demagnetization was performed on companion samples for the Naude's Nek section only. Magnetic susceptibility was monitored in parallel with heating experiments, in order to calculate the Koenigsberger ratio and to detect mineralogical changes upon demagnetization. Better quality results were obtained by thermal demagnetization, which was more effective in isolating the characteristic magnetization. This is especially true for transitional samples which have often suffered a larger overprint than during full polarity intervals, due to the low strength of the transitional field. We also noted the presence of high-coercivity minerals in some samples, likely some hematite with zero or low Ti content. All results are for thermally demagnetized samples with at least 8 successive heating steps. Less than 5% of the samples did not yield any characteristic direction and were rejected (involving only 7 sites out of 185). In most cases, we suspect that these sites have been affected by lightning.

[14] Figure 2 shows four characteristic examples of thermal demagnetization vector diagrams of samples with transitional directions (using *Cogné*'s [2003] software). In all cases, a uni-vectorial component can be isolated beyond 400°C. A significant amount of magnetization beyond the Curie temperature of magnetite sometimes remained in samples from Moteng-Pass, suggesting the additional presence of hematite (consistent with af demagnetization characteristics). Directions of magnetization were the same for both phases and consistent with overlying flows, hence we infer an early origin for the two components, acquired during cooling of the lava flow. A few samples (~9% of all samples, 24% of transitional samples) displayed more complex

Table 2. Distinct Transitional Magnetic Directions From the Naude's Nek, Oxbow-Moteng Pass and Bushmen's Pass Sections[a]

Directional Group or Single Flow	Site(s)	N	Dg (deg)	Ig (deg)	K	α_{95} (deg)
		Naude's Nek Section				
DG16	NN38,NN40	16	4.5	4.5	512.6	1.7
DG15	NN42, NN44, NN45	24	356.2	18.1	75.3	3.4
14	NNPR	9	24.1	−49.3	64.7	6.5
DG13	NN46, NN47	15	54.6	−53.9	57.4	5.1
12	ND49	8	39.5	−56.1	54.6	7.9
DG11	ND51 to ND53	24	2.9	−12.2	57.2	4.0
10	ND54	7	350.3	−44.7	54.4	8.8
DG9	ND55, ND56	15	1.5	−12.2	129.2	3.5
8	ND57	8	357.1	−29.7	90.5	6.4
DG7	ND58, ND60	14	358.6	−19.4	54.9	5.5
		Oxbow-Moteng Pass Section				
OM11	MP24	8	68.2	−68.3	189.5	4.0
OM10	MP23	7	86.2	−70.9	274.2	3.7
OM9	MP22	8	64.3	−69.0	612.7	2.2
DG-OM8	MP20, MP21	14	96	−74.5	132.9	3.5
OM7	MP19	7	38.8	−63.1	104.0	5.9
OM6	MP18	6	6.4	−40.0	89.4	7.1
DG-OM5	MP15 to MP17	22	117.5	20.4	64.0	3.9
OM4	MP13	7	135.7	23.2	198.3	4.3
		Bushmen's Pass Section				
29	X26, R1, R2, R3, R4	18	4.3	−19.2	70.0	3.9
28	X25	5	1.9	−53.1	117.0	7.1
27	X23B, X24	8	7.0	−33.3	39.0	9.0
26	X23A	5	350.2	−47.7	64.0	9.6
25	X21	6	7.5	−33.1	49.0	9.7
24	X20	9	356.7	−31.2	76.0	5.9
23	X19	8	19.2	−59.5	54.0	7.6
22	X16, X17, X18	28	46.5	−63.0	226.0	1.8
21	X14, X15	11	93.5	−69.6	123.0	4.1
20	X12, X13	13	71.0	−78.1	113.0	3.9
19	X11	3	344.8	−67.6	318.0	6.9
18	X10	4	50.0	−73.6	376.0	4.7
17	X9	5	58.6	−70.9	184.0	5.7
16	X8	6	356.5	−15.6	275.0	4.0
15	X7	3	347.8	−33.0	448.0	5.8
14	X6	8	9.3	−5.6	81.0	6.2
13	X5	5	343.3	−46.1	53.0	10.6
12	X4	5	5.5	−23.8	75.0	8.9
11	Z7, Z9, Z10, X1, X2, X3	35	121.5	27.7	340.0	1.3
10	Z6	4	117.3	28.8	621.0	3.7
9	Z5	6	121.3	34.4	225.0	4.5

[a]DGx (for the Naude's Nek section) or DG-OMx (for the Oxbow-Moteng Pass section) is for a directional group, and X (for the Naude's Nek section) or OMx (for the Oxbow-Moteng Pass section) is for a single flow. N represents the number of samples defining the cooling unit. Other column headings are the same as those in Table 1. Bushmen's Pass section directions are from *Prévot et al.* [2003].

behavior upon demagnetization, but the characteristic component could always be determined using great circle analysis [*McFadden and McElhinny*, 1988].

[15] Site/flow mean directions are listed in Table 1 and four examples are shown in stereographic projection in Figure 3; the mean directions for the two stable polarity chrons [*Moulin*, 2011; *Moulin et al.*, 2011] are shown for reference. Apart from very few clear outliers that were rejected (e.g., for site MP13; only 1 sample out of 8), sample directions are seen to be rather well grouped: 6 out of 35 mean directions have confidence intervals between 10 and 13° and are not considered further in the study. When directional group (DG) averages are calculated (see below and Table 2), 10 out of 18 have confidence intervals less than 5° and 8 are

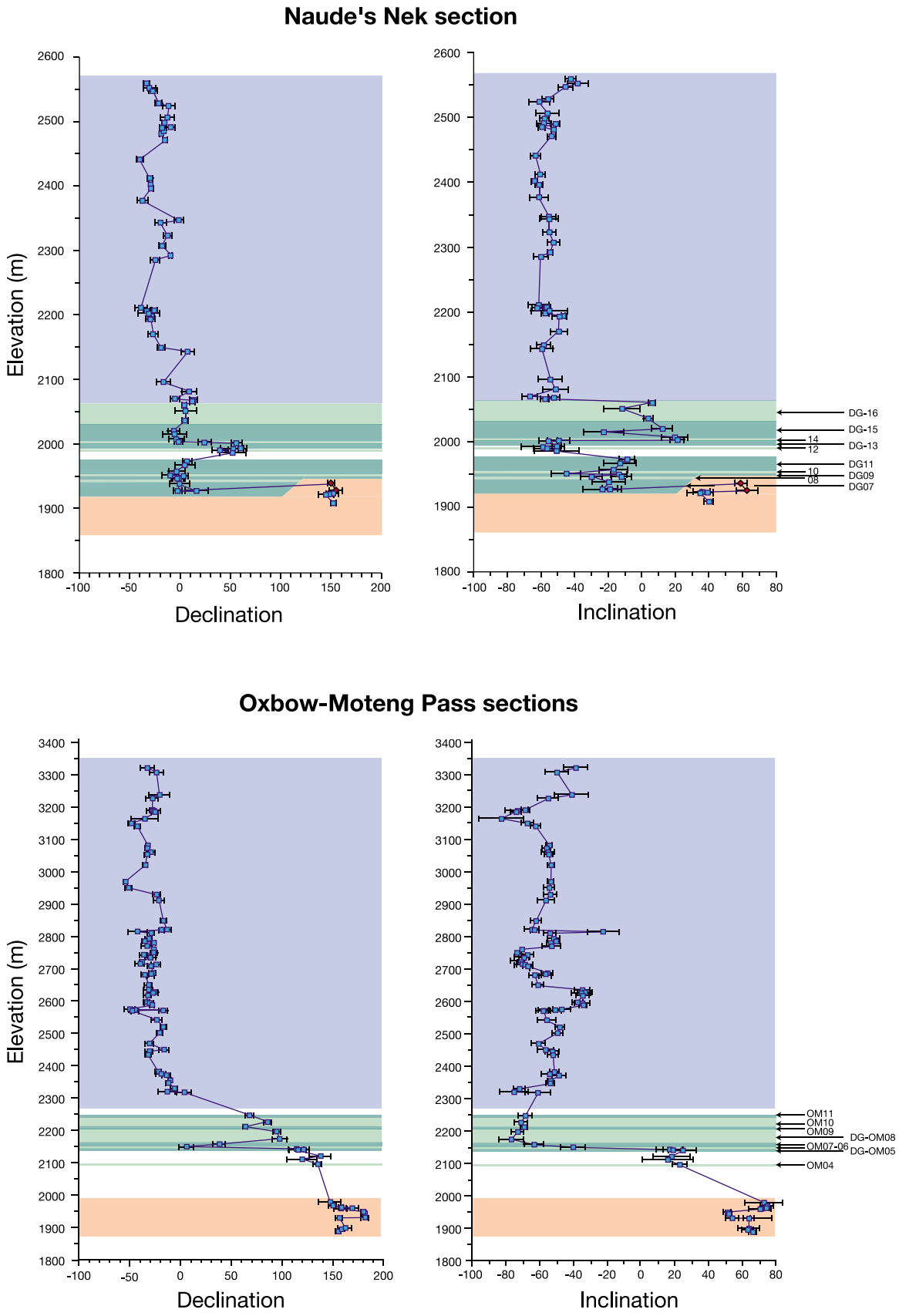

Figure 4

between 5 and 9°. All characteristic directions retained for the final compilation are of good quality and there is little doubt that they are primary and accurate.

[16] The mean declinations and inclinations calculated for the successive flows in each sequence are shown in Figure 4. In the Naude's Nek section, the transition begins by an abrupt switch of declination from south to north, followed by a rebound to values of about 60° with steep inclinations; declination next remains close to 0° while inclination goes back to shallow values before completing the transition. The Oxbow-Moteng Pass combined section has recorded a more progressive evolution of transitional directions. The onset of declination changes is smoother but a rapid jump to northward directions follows. In a second phase, as in the Naude's Nek section, a rebound occurs, this time toward declinations close to 90° associated with inclinations up to almost 80°.

2.3. Directional Groups

[17] We recall the concept of directional groups (DG) which we have used extensively in studies of LIP volcanism [e.g., *Chenet et al.*, 2008, 2009]. Whenever the directions of two flows, overlying each other in direct succession, are statistically undistinguishable, we interpret this as the sign that there has not been enough time between the cooling of the two lava flows to have recorded significant changes due to secular variation of the geomagnetic field. Under the assumption that the recent (archeomagnetic) field provides good estimates of the root mean square velocity of secular variation (on the order of 3° per century [e.g., *Chenet et al.*, 2008] (based on *Gallet et al.* [2003])), we interpret this as a sign that the two flows were actually part of the same larger cooling unit that was erupted in, say, less than a century and we average the directions together. We apply this only to reasonably well determined paleomagnetic site directions, i.e., with a confidence level α_{95} less than 10° (Table 2). *Mankinen et al.* [1985] were probably the first to use this concept on the Columbia River LIP, followed by *Jarboe et al.* [2008]. *Riisager et al.* [2002, 2003] used it for the North Atlantic Tertiary Volcanic Province, *Knight et al.* [2004] for the Central Atlantic Magmatic Province, *Chenet et al.* [2008, 2009] for the Deccan traps, *Heunemann et al.* [2004] and *Pavlov et al.* [2010] for the Siberian traps and *Kosterov and Perrin* [1996] and *Prévot et al.* [2003] for the Karoo LIP itself. This has allowed the identification of huge volcanic pulses with volumes in excess of 1000 km^3 [e.g., *Chenet et al.*, 2008, 2009]. When discussing transitional directions of the Karoo LIP sections below, we use the directional groups identified and calculated as above plus all single flow directions that could not be associated with those of the immediately underlying and overlying flows (Table 2). Note that, because dipole field intensity is generally lower during the directional reversal, the root mean square velocity of secular variation could be significantly larger than 3° per century, hence the size of directional groups correspondingly larger.

2.4. Transitional Directions

[18] The two mean directions and poles for reversed and normal sites pass a class B reversal test [*McFadden and McElhinny*, 1990] and are close to and consistent with previous determinations by *van Zijl et al.* [1962a, 1962b], *Kosterov and Perrin* [1996] and *Hargraves et al.* [1997] and to the synthetic poles for Africa in the 175–185 Ma range by *Besse and Courtillot* [2002]. The overall mean direction based on the mean magnetic directions of all directional groups and individual lava flows in the three sections, excluding transitional directions, is at D = 336.4°, I = −56.5° (N = 44, α_{95} = 3.5°) and the VGP at lat = 68.9°N, long = 268.1°E (A_{95} = 4.3°). For more details see *Moulin* [2011] and *Moulin et al.* [2011].

[19] As far as transitional directions are concerned, we first determined VGPs for each site mean direction, and then determined approximately the beginning and end of the transition zone. Because the Jurassic pole is not at the present pole, we rotated the mean pole from all "fully" normal and reversed directions to the present geographic pole. We identified final transitional directions in this new reference frame using a cutoff latitude of 60°

Figure 4. Stratigraphic logs of site mean declination and inclination for the Naude's Nek and Oxbow-Moteng Pass sections as a function of altitude. Reversed directions are outlined with a pink band, transitional directions by a green one, normal directions by a pale blue band. All site means are shown and directional groups are indicated with their name by arrows. The Naude's Nek section actually results from splicing two separate sections (Bell River traverse in blue and Adjacent Valley traverse in red) hence the apparent stratigraphic discrepancies at the bottom of the section (full details given by *Moulin et al.* [2011]).

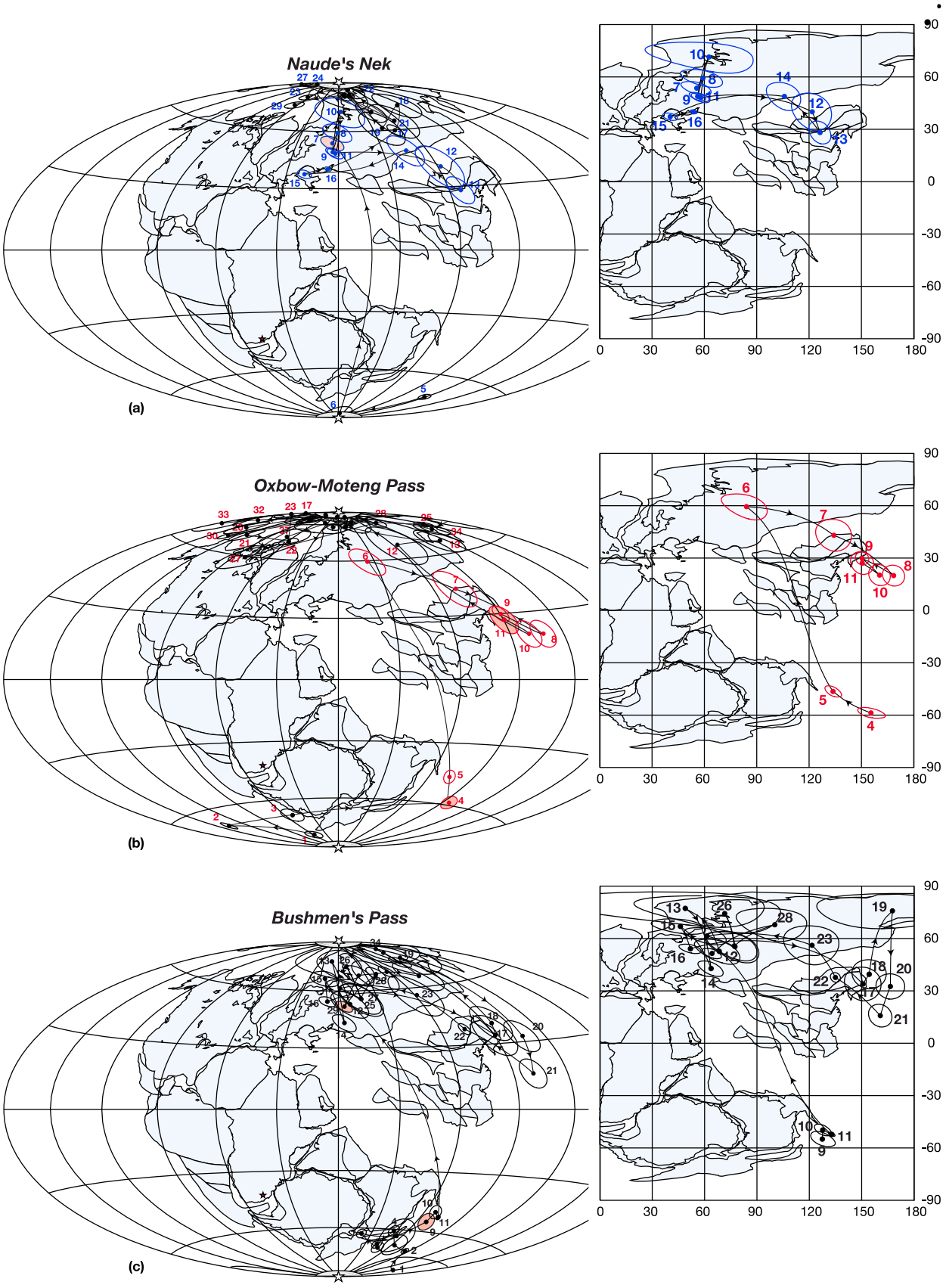

Figure 5

[e.g., *McElhinny and Merrill*, 1975] (other cutoff values and definitions were used which did not change the results and are therefore not discussed here). This is also consistent with the amplitude of secular variation prior to and after the reversal (Figure 4). We took into consideration the possibility of rebounds to reverse or normal polarity. Results are shown in Figure 5a for the Naude's Nek section and in Figure 5b for the Moteng Pass section (the mean full polarity poles for the rest of the sections are shown as open stars).

[20] We have determined 23 transitional directions and therefore poles in the Naude's Nek section (Figure 5a and Table 1). The total thickness of the transitional lavas is 130 m. The magnetic recording actually reveals only 10 independent directions (4 individual directions and 6 directional groups as defined above), leading to poles numbered 7 to 16 in Figure 5a (the last "fully" reversed pole is 6 and the first "fully" normal one is 17). There is no observed transitional VGP close to reversed polarity and the first recorded direction is already in the "normal hemisphere." The reversal trajectory begins (7 to 11) with a series of 3 confined, polarized hairpins: latitudes range from 45 to 62°N but longitudinal range is less than 4°. The path continues with a narrow loop (12 to 14) to the South-East, down to 26° in latitude. VGPs return close to their previous position (15 and 16) before completing the reversal.

[21] *Prévot et al.* [2003] sampled part of the Naude's Nek section and we were able to find the holes from one of their sites, which we resampled as site NNPR. Our direction is fully compatible with Prévot et al.'s direction for site RH8 and we could unambiguously correlate their sites RH4–5 (a DG) and RH7 to our sites 11, 13 and 14 [see *Moulin et al.*, 2011].

[22] In the Moteng Pass section, we found 13 transitional sites, corresponding to 8 distinct magnetic directions (2 DGs and 6 individual flows) and 160 m of lava thickness (Figure 5b). Two VGPs (4 and 5) are close to reversed polarity and mark the onset of the reversal, not recorded in Naude's Nek. The pole jumps to the normal hemisphere (6), describes a narrow loop to the South-East (6 to 12) down to 23°N with two small but sharp and polarized hairpins (15° latitude range, only a few degrees across track). VGP 12 is the first normal pole in the new chron.

[23] The two recordings of the reversal, which are ~200 km apart, are consistent and complementary. They share a number of features: 1- a large directional jump with no transitional poles between 45°S and 45°N at the time of equatorial crossing, 2- a large thin loop to the SE with poles going down to ~20° latitudes, and 3- a rebound to normal polarity then to low latitudes before finally settling in this normal polarity state. We return to this observation and integrate earlier results from other studies in section 4.

3. Relative Transitional Paleointensities From the Naude's Nek and Moteng Pass Sections

[24] A complete description of the reversing field requires the modulus of the vector: this has critical importance during a reversal. Because of the large number of samples involved and the time-consuming experiments that would be required for absolute paleointensity measurements, we have only determined relative paleointensities. Similarly, *van Zijl et al.* [1962a, 1962b] and *Prévot et al.* [2003] used a cleaned remanence intensity (either by a 10 mT field or heating at 200°C), arguing that this seemed reasonable considering the petrographic monotony of the lava and the relative weakness of the secondary components. Because we found evidence of several magnetic phases and different demagnetization behaviors, it may not be acceptable to mix all remanence intensities obtained at the same step of cleaning without any parameter that would compensate for these differences. In addition, values should be normalized with respect to the concentration of magnetic material involved in the remanence.

[25] We followed a more demanding approach, in the light of experience acquired in studies of relative paleointensities in sediments and taking

Figure 5. Virtual geomagnetic poles for the (a) Naude's Nek and (b) Oxbow-Moteng Pass sections (this paper) and (c) Bushmen's Pass section [*Prévot et al.*, 2003]. Poles are numbered in stratigraphic order. The first and last transitional poles are shown with pink 95% uncertainty circles (note that the uncertainty circle for the last transitional pole, number 16, in Naude's Nek is too small to be visible). The transitional poles are shown again on a Mercator projection on the right for clarity. The mean Lesotho Jurassic pole (calculated using all directional groups and individual lava flows from the Naude's Nek, Oxbow-Moteng Pass and Bushmen's Pass sections, excluding transitional directions) is used as reference and rotated to the coordinate system north pole and continents are shown (pale blue) in their Jurassic positions (see text). The sampling site is shown as a red star.

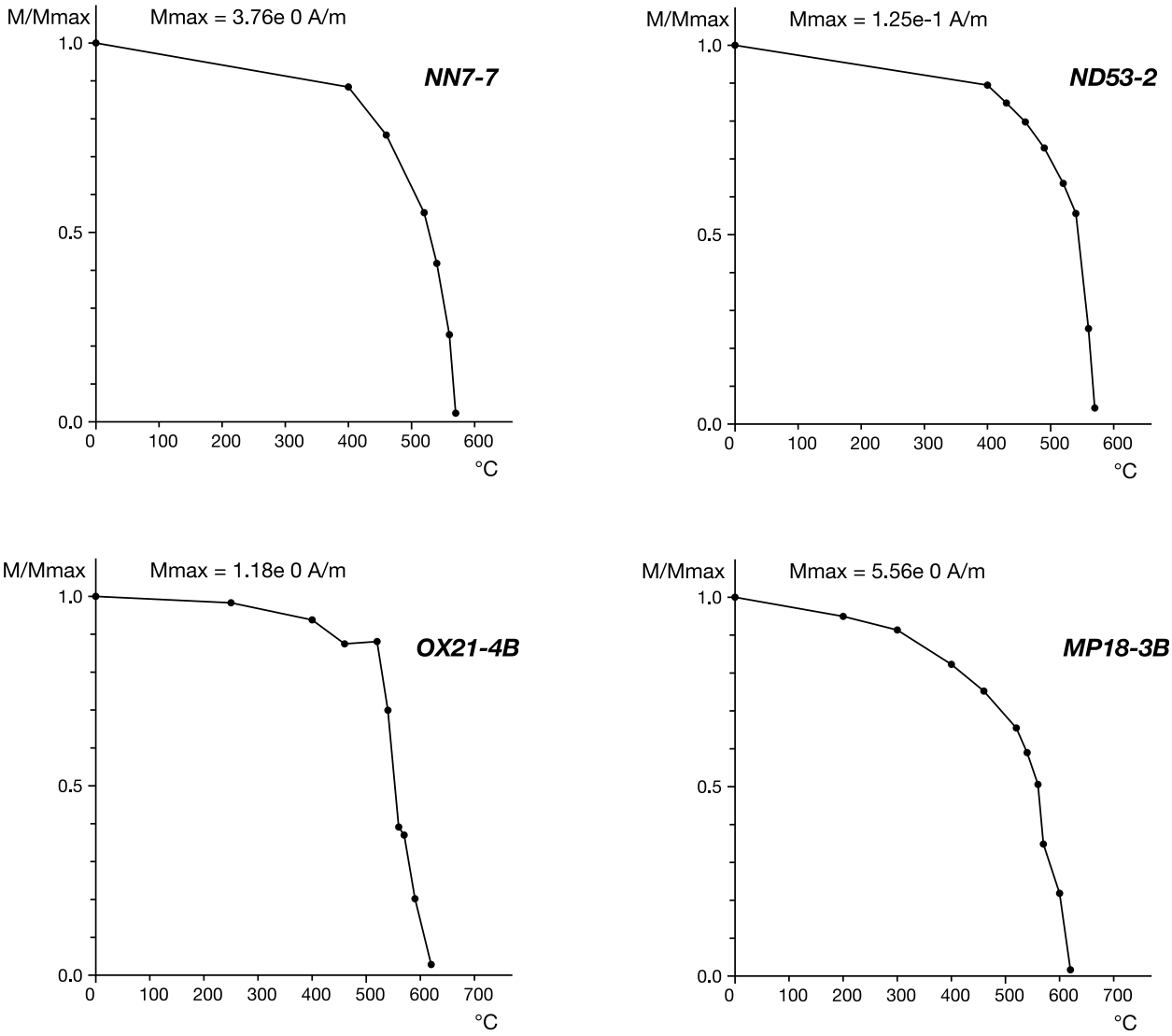

Figure 6. Four representative thermal demagnetization diagrams of samples from the Naude's Nek (NN, ND) and Oxbow-Moteng Pass (OX, MP) sections selected for measurement of relative paleointensity as explained in the text.

advantage of recent work [*Herrero-Bervera and Valet*, 2009; *Valet and Herrero-Bervera*, 2011], in which it is argued that rigorous pre-selection of samples can lead to almost 100% success rate in classical Thellier-Thellier experiments of absolute paleointensity: this pre-selection involves samples with magnetization carried by single-domain grains of pure magnetite (possibly with minor amounts of hematite with the same magnetization history and direction). These can be identified according to their behavior upon thermal demagnetization (examples are shown in Figure 6): a rapid decrease of the initial magnetization by at least 70% over a narrow range of high temperatures just below the Curie point. In other words, we have selected samples with a well-defined characteristic component decreasing toward the origin of the demagnetization diagrams beyond at least 450°C. Although satisfying these criteria significantly reduces the number of useable samples, we find it more rigorous to extract a suitable evolution of the field from a few determinations, rather than dealing with scattered variations derived from a larger number of specimens. In the present study, this selection left us with 18 samples from Naude's Nek and 27 from Moteng Pass. The NRM above 500°C was normalized by the full TRM (obtained after in-field heating of the samples beyond 580° C) or by TRM_{520} defined as the "full" TRM remaining after zero-field heating at 520°C. The relative paleointensities obtained in each section by these techniques are shown in Figures 7a and 7b

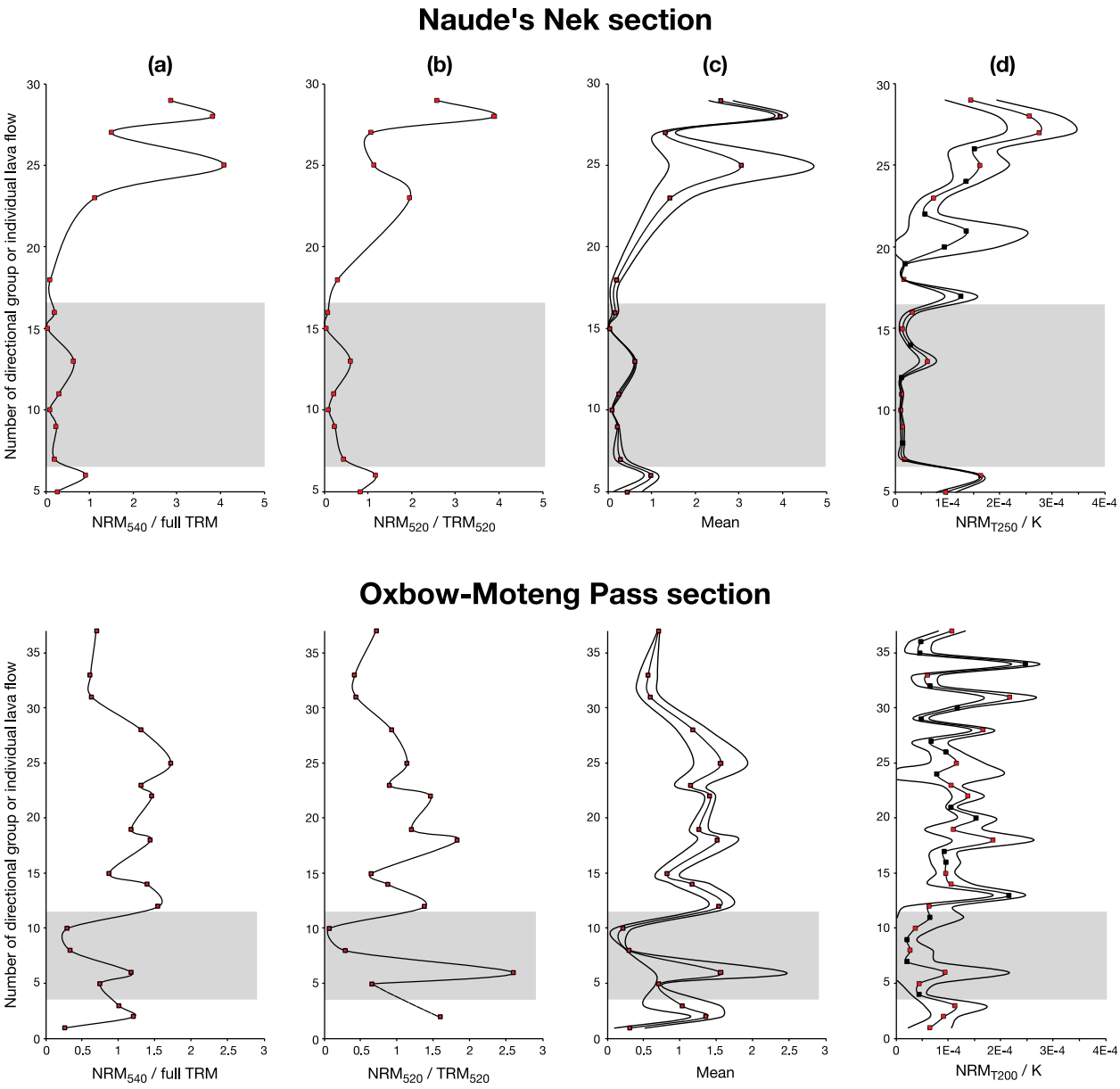

Figure 7. Relative paleointensity determinations for selected samples from the (top) Naude's Nek and (bottom) Oxbow-Moteng Pass sections. The ratios used (see text) are (a) NRM after heating to 540°C in zero field normalized by full TRM, (b) NRM after heating to 520°C in zero field normalized by TRM remaining at 520°C upon cooling in zero field, (c) average of the two previous data sets plus a third one (not shown) NRM after heating to 520°C in zero field normalized by full TRM, and (d) the more conventional but less robust estimate TRM remaining at 250°C (for Naude's Nek; 200°C for Oxbow-Moteng Pass) upon cooling in zero field over magnetic susceptibility K.

for the ratios NRM_{540}/fullTRM and NRM_{520}/TRM_{520}. The curves are similar, though we note differences in amplitudes at some levels. In order to take those into consideration, we have averaged three different estimates (NRM_{520}/fullTRM; NRM_{540}/fullTRM and NRM_{520}/TRM_{520}); the resulting variations are seen in Figure 7c (transitional intervals are shown in gray): they represent our preferred approximation of field intensity changes throughout the reversal in the two sections, and can be interpreted within the limits shown by the uncertainties. The standard deviations remain small in both sequences, giving us confidence about the geomagnetic origin of field changes across the reversal. For comparison, we have plotted in Figure 7d the NRM "cleaned" at 250°C for the Naude's Nek section and at 200°C for the Oxbow-Moteng Pass section, both

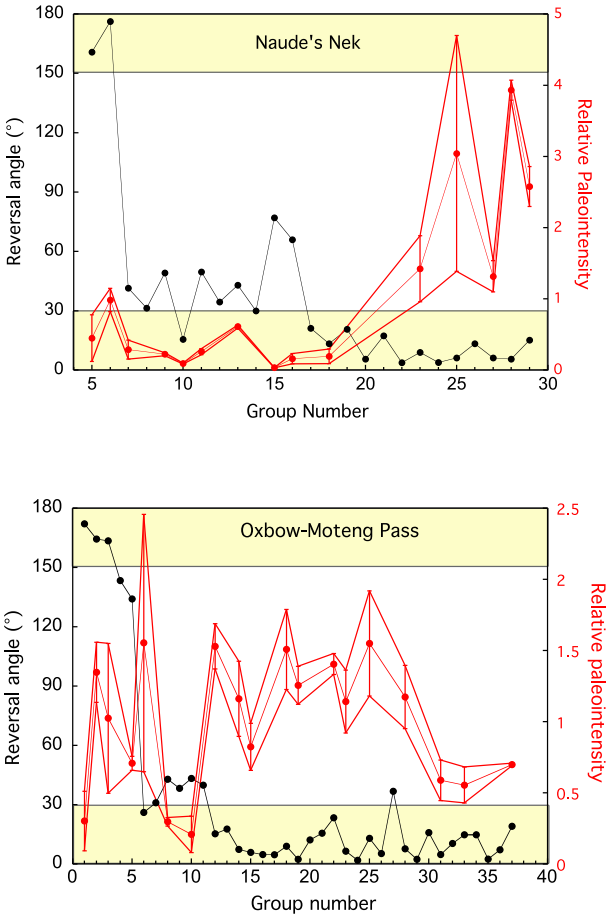

Figure 8. Reversal angle and relative paleointensity (as in Figure 7c) as a function of (directional) group number in stratigraphic order. Transitional directions correspond to reversal angles between 30 and 150°; pale yellow bands indicate full polarities.

normalized by low-field magnetic susceptibility (NRM_{T250}/K or NRM_{T200}/K) for all samples, i.e., without any pre-selection. This of course yields more numerous data (since all flows can be used) but results may be less robust, since K is also sensitive to magnetic grains other than those entering the natural remanence. The results appear globally similar (Figure 7c versus Figure 7d) with some differences, particularly after the transitional zone. Finally, these different approaches yield consistent characteristics of field evolution across the reversal.

[26] The reversed and normal polarity samples from the Naude's Nek section have an intensity one order of magnitude larger than that of transitional samples. The overall pattern of the changes suggests recording of a weakened reversed field prior to the (directional) reversal, a much lower intensity during the transition and a gradual recovery after the reversal, with eventually normal directions with intensity 10 times larger than during the transition itself. In the Moteng Pass section, we have very few samples from the lower reversed interval. There is one high intensity point within the transitional zone but it is mainly due to the estimate at 520°C which is much larger than at 540°C (resulting in a large uncertainty at that point in Figure 7c), and thus may not be robust. The Moteng Pass section gives a more subdued message than that at Naude's Nek, but both messages are consistent. Based on the VGP paths of Figure 5, the Moteng Pass section would have recorded early phases of the transition not recorded in Naude's Nek. The remaining dispersion of the data in Figure 7d is likely due to variations in magnetic mineralogy, concentration and grain size. In summary, the patterns emerging from Figure 7 argue for a transitional intensity that has decreased by ~80% in Moteng Pass and ~90% in Naude's Nek with respect to full polarity values.

[27] We can compare the evolutions of the "reversal angle" (the angular distance between the mean paleomagnetic direction of each flow or cooling unit and the direction of the normal field) and of relative field intensity as a function of group number in Figure 8, which allows us to analyze the dynamical (vector) pattern of the transition without reference to VGPs. At Naude's Neck, field intensity is already low immediately prior to the reversal and remains weak during the entire transitional period. Interestingly, there is a first small field recovery recorded by group 13 but then intensity drops again while the direction returns to transitional values (which correspond to the low latitude VGPs of the excursional phase in Figure 5a). This succession reflects an aborted recovery of the dipole toward the new polarity, followed by a rebound to a transitional state with very low field intensity prior to final recovery in the new polarity.

[28] The same features are present at Oxbow-Moteng Pass, particularly the short episode of partial recovery prior to the weak intensities associated with the rebound, both being better documented in the latter section, where normal polarity has been recorded by more lava flows. A similar structure, with a rapid polarity change followed by a rebound, has been reported in several detailed reversal records [*Chauvin et al.*, 1990; *Herrero-Bervera and Valet*, 1999; *Herrero-Bervera et al.*, 1999; *Riisager and Abrahamsen*, 2000]. These successive episodes are reminiscent of present-day field changes linked to secular variation of the non-dipole field but with a much larger amplitude, which is readily

understood as a consequence of the decrease in axial dipole intensity.

4. Reconstruction of the Reversal Path and Discussion

[29] The two new reversal paths produced by the present study (Figures 5a and 5b) and the one recorded at Bushmen's Pass (Figure 5c) by *Prévot et al.* [2003] can now be compared. We are in the rather unique position that we have three independent and rather detailed recordings of the same reversal by three thick lava sections that are both distant enough (Naude's Nek-Bushmen's Pass = 125 km; Bushmen's Pass-Moteng Pass = 95 km; Naude's Nek-Moteng Pass = 195 km; see Figure 1) that they can be considered independent, yet close enough to have recorded the same core field (dipolar plus non-dipolar terms). It is clear from Figure 5 that the three records are compatible and complementary at the same time. They can therefore be blended into a single path (Figure 9).

[30] The beginning of the reversal is recorded only in Moteng Pass (MP) and Bushmen's Pass (BP). The first five transitional poles from the two sections appear to form a secular variation loop. The VGPs then jump by 120°. Five poles from Bushmen's Pass (12 to 16, in black, inset in Figure 5c) and 5 poles from Naude's Nek (NN, 7 to 11 in blue, inset in Figure 5a) form two quite similar sets of double hairpins, confined in longitude. The poles then jump to the East and form a large multiple hairpin loop, in which poles from the three sections can be integrated in a consistent way (Figure 9). The Bushmen's Pass section has two hairpins that return the field to a full axial dipolar direction (Figure 5c, poles 19 and 23 in black). The apices of 8 sub-parallel segments that form the back and forth tracing hairpins are (Figure 5) at OM6 (red, onset of the full secular variation loop), BP17 (black), BP19 (black), DG-OM8 (red), OM9 (red), BP21 (black), BP23 (black), DG13 (blue) and DG15 and DG16 (blue, end of the full secular variation loop). The hairpins end close to the cloud of poles where they started near (60°N, 60°E) (arbitrary longitudes in Figure 5). In summary, the reversal path is composed of a first transit from quasi-reversed to quasi-normal directions, followed by a large excursion (rebound) with multiple hairpin structure ending in normal polarity.

[31] Distant correlations can be established between sections based on similar magnetic directions of either individual flow directions, directional groups, or hairpins identified in Figure 9 [see *Moulin*, 2011]. Note that the onset of the reversal is missing from Naude's Nek; a pause in volcanic activity must have occurred between directions/flows 6 and 7 (Figure 5a, inset). There is an observational gap in Moteng Pass that has prevented observation of the end of the large hairpin loop.

[32] As in many volcanic records [e.g., *Prévot et al.*, 1985; *Hoffman*, 1992; *Riisager et al.*, 2002; *Valet and Herrero-Bervera*, 2003; *Heunemann et al.*, 2004], the reversal path shows VGP clusters, directional jumps between clusters, loops and hairpins and a lack of low-latitude VGPs. An important issue regarding the reversal mechanism would be to identify the origin of these characteristic features: do they reflect volcanic or geomagnetic processes? Turning to Figure 9, could the transitional poles at the onset of the reversal reflect a short-lived episode of intense volcanism, an actual secular variation loop or a longer pause with a preferred field direction influenced by the core-mantle boundary? How fast is the first transit in the reversal path, with no intermediate pole between 45°S and 45°N? Does it imply a pause in volcanism? Is the (quasi-normal) cloud of poles around (60°N, 60°E), where the second part of the reversal with the large elongated hairpin loop toward the South East starts and ends, a long-standing feature of the transitional field?

[33] In general, the uncertainties on radiometric ages (∼1%) prevent a direct solution of these questions. We can however formulate some hypotheses, based on (1) expected features of secular variation during a reversal dominated by the non-axial dipole field, (2) the observation of paleomagnetic directional groups, (3) evolution of paleo-intensity within the reversal, (4) the occurrence of sedimentary layers occurring between certain lava flows and (5) the statistics of low latitude transitional VGPs in other reversal records.

[34] (1) Instantaneous VGP drift rates resulting from secular variation could have been quite large during the directional part of the reversal record, because the field was quite weak and likely non-dipolar. The time constants of degree n non-dipolar terms vary roughly as $1/n$ and for instance the typical time constant of the quadrupolar field is on the order of 250 years [*Hongre et al.*, 1998]. The ∼100° jump in VGP directions in the main part of the reversal might therefore represent no more than a few centuries.

[35] (2) Narrow groups of magnetic directions (and poles) corresponding to sequences of lava flows have been observed in many LIPs and have been

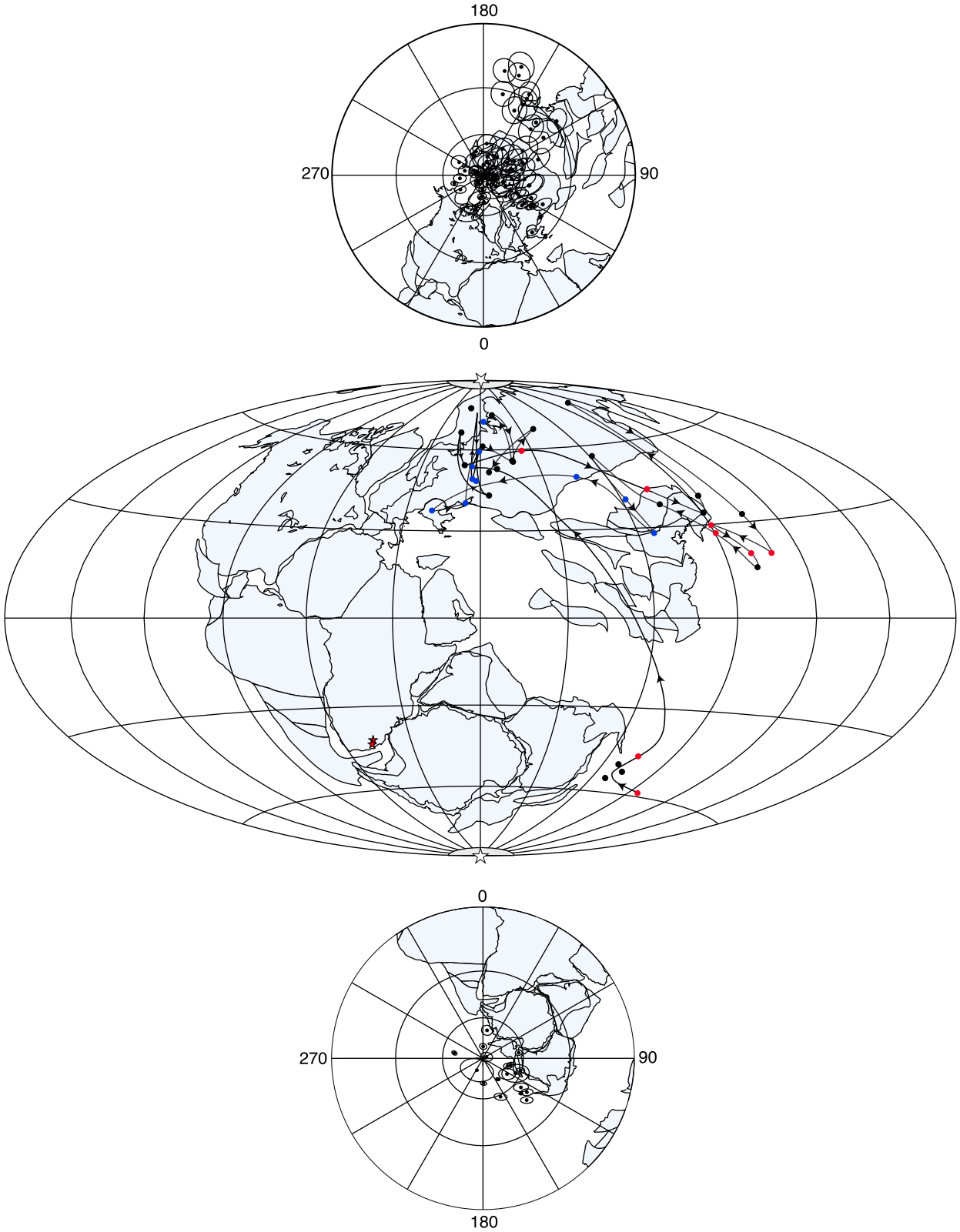

Figure 9. Integration of the three VGP (transitional) reversal paths of Figure 5 into a single composite one. Blue poles are from Naude's Nek, red poles from Moteng Pass (this study) and black ones from Bushmen's Pass [*Prévot et al.*, 2003]. Polar projections of (middle) only transitional VGPs and (top and bottom) all VGPs (reverse, transitional and normal). Sampling sites shown as red stars.

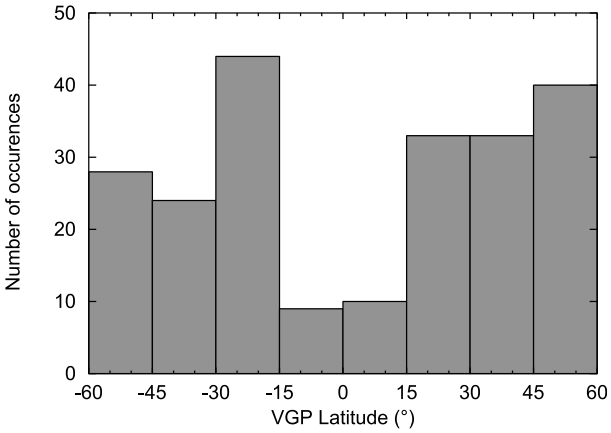

Figure 10. Histogram of VGP latitudes: this compilation includes results from *Chauvin et al.* [1990], *Coe et al.* [2004], *Herrero-Bervera and Valet* [1999], *Herrero-Bervera et al.* [1999], *Mankinen et al.* [1985], and *Riisager et al.* [2002].

interpreted in terms of magmatic pulses, i.e., intense volcanism over a period of time short enough to have prevented the recording of paleosecular variation. Based on earlier work on such magmatic pulses in the Deccan LIP [*Chenet et al.*, 2008, 2009] and on the rest of our work on the Karoo LIP [*Moulin*, 2011; *Moulin et al.*, 2011], we propose that many of these directional groups could indeed indicate large yet rather brief magmatic pulses. We note again that the characteristic size of these DGs could be significantly larger during the reversal than during full polarity states due to the decrease in dipole field intensity.

[36] (3) Some authors [e.g., *Hoffman and Singer*, 2008] propose that clusters (larger than the above directional groups) might correspond to long-lived features in the core field if they result from the restoration of a dipolar configuration, which would be accompanied by larger paleo-intensities. The fact that a subset of poles prior to and just after the second part of the reversal, i.e., the hairpin with the rebound to SE transitional directions, are located in similar regions might argue in favor of a preferred location of the reversing field (although these clusters are almost non-transitional in VGP latitude). Similar clusters with preferred, recurrent locations are seen in some sedimentary sequences and in dynamo simulations [*Olson et al.*, 2011]. On the other hand, *Valet and Plenier* [2008] find that such dense VGP clusters can simply result from a simple time-varying non-dipolar transitional field. Also, the relative intensities of our samples in the separate parts of each section that correspond to each cluster do not show strong evidence for an increase in field intensity in these clusters, contrary to what is found for instance by *Heunemann et al.* [2004] in the 250 Ma old Siberian traps. These relative intensities are therefore not indicative of a stronger dipolar field. These conclusions should however be regarded with caution given the size of the uncertainties (Figure 8).

[37] (4) When analyzing the Bushmen's Pass results, *Prévot et al.* [2003] suggested that the main directional jump was associated with a pause in volcanic activity, based on the observation of an intervening sedimentary horizon. We have also found that a sedimentary level occurs in our two sections at the time of the main VGP jump (phase 1 of the reversal). Actually, 6 sedimentary layers with a thickness between 1 and 2 m, all located at the level of the reversal, have been identified in Moteng Pass (3 between OM4 and DG-OM5, 1 between DG-OM5 and OM6 and 1 between OM7 and DG-OM8). Except for the jump between DG-OM5 and OM6, no other VGP jump associated with an intervening sedimentary horizon in any section has such a large amplitude (though these sedimentary horizons are similar). In Naude's Nek, there are 7 sedimentary horizons: one just before the onset of the reversal (before DG7 [*Moulin et al.*, 2011]) and a single one within the reversal. Three of these horizons are within directional groups (2 in DG2 and 1 in DG16) and have therefore likely been formed in a short period of time. The one before DG7 is simply a 10 m long, 10 to 30cm thick lens. All the sedimentary levels we have observed in the NN and MP sections are detrital sandstones with unknown lateral extent in several cases; they may have resulted from eolian erosion of the underlying Clarens formation. In conclusion, though it is obvious that the deposition of these sedimentary horizons does require some time to form, this duration cannot be determined and can be argued in many cases to have been quite short. Therefore, it may not imply a long pause in volcanic activity.

[38] (5) We note that reversing VGPs are seldom located at low latitudes [*Love*, 1998; *Valet and Herrero-Bervera*, 2003; *Heunemann et al.*, 2004; *Leonhardt and Fabian*, 2007]. The compilation of latitudes of reversing VGPs shown in Figure 10 indeed has very few poles under 15° latitude. Such is the case for the "van Zijl" reversal (Figures 5 and 9).

5. Conclusion

[39] In this paper, we have reported new paleomagnetic results from two thick continuous

sequences of flood basalts of the Karoo large igneous province. Using the concept of directional groups (which have recorded essentially the same paleo-field over what we argue is likely a short cooling time, less than about a century), we have identified 10 independent directions over 130 m in the Naude's Nek section and 8 over 160 m at Moteng Pass. Relative paleo-intensities from a careful selection of magnetically well-behaved samples indicate a low paleo-field intensity prior to the directional changes and a progressive recovery to the following normal polarity. Transitional intensity was 80 to 90% lower than full polarity values. Our two VGP reversal paths can be combined with a third one, previously obtained by *Prévot et al.* [2003]: the three paths are consistent and complementary and a single composite path has been constructed from them (Figure 9). The poles transit early in the sequence to almost normal polarities, then rebound to lower latitudes (∼20°), return to their previous position close to the normal state (but with weak intensities) and then finally settle in normal polarity. Despite the lack of detailed chronologic markers, the absence of transitional VGPs during the initial S to N transit is in contrast to the following rebound (multiple hairpin loop) which has a complex structure and is documented by many poles. We suggest that this (main?) phase of the reversal occurred very rapidly. The ∼180 Myr old "van Zijl" reversal shares many characteristics with more recent reversals up to the latest one, Brunhes-Matuyama. There is no indication that features in the dynamo processes which produce these reversals have changed much in the past 200 Myr.

Acknowledgments

[40] This work was supported by Conseil Régional d'Ile de France and the French Ministry of Foreign Affairs in the frame of an ARCUS program with South Africa, and by CNRS in the frame of a joint International Program with South Africa entitled *!Khure Africa.* The authors are particularly indebted to Julian Marsh from Rhodes University for guidance in the field. VC is grateful to his South African co-chair of *!Khure Africa*, Maarten de Wit, for continued support. We thank the reviewers for comments on the manuscript. This is IPGP contribution 3271.

References

Barton, C. E., and P. L. McFadden (1996), Inclination shallowing and preferred transitional VGP paths, *Earth Planet. Sci. Lett.*, *140*, 147–157, doi:10.1016/0012-821X(96)00025-8.

Besse, J., and V. Courtillot (2002), Apparent and true polar wander and the geometry of the geomagnetic field over the last 200 Myr, *J. Geophys. Res.*, *107*(B11), 2300, doi:10.1029/2000JB000050.

Brown, M. C., R. Holme, and A. Bargery (2007), Exploring the influence of the non-dipole field on magnetic records for field reversals and excursions, *Geophys. J. Int.*, *168*, 541–550, doi:10.1111/j.1365-246X.2006.03234.x.

Channell, J. E. T., and B. Lehman (1997), The last two geomagnetic polarity reversals recorded in high deposition-rate sediments drifts, *Nature*, *389*, 712–715, doi:10.1038/39570.

Chauvin, A., R. A. Duncan, N. Bonhommet, and S. Levi (1989), Paleointensity of the Earth's magnetic field and K-Ar dating of the Louchadière volcanic flow (central France): New evidence for the Laschamp excursion, *Geophys. Res. Lett.*, *16*(10), 1189–1192, doi:10.1029/GL016i010p01189.

Chauvin, A., P. Roperch, and R. A. Duncan (1990), Records of geomagnetic reversals from volcanic islands of French Polynesia: 2. Paleomagnetic study of a flow sequence (1.2–0.6 Ma) from the island of Tahiti and discussion of reversal models, *J. Geophys. Res.*, *95*(B3), 2727–2752, doi:10.1029/JB095iB03p02727.

Chenet, A. L., F. Fluteau, V. Courtillot, M. Gérard, and K. V. Subbarao (2008), Determination of rapid Deccan eruptions across the Cretaceous- Tertiary boundary using paleomagnetic secular variation: Results from a 1200-m-thick section in the Mahabaleshwar escarpment, *J. Geophys. Res.*, *113*, B04101, doi:10.1029/2006JB004635.

Chenet, A. L., V. Courtillot, F. Fluteau, M. Gérard, X. Quidelleur, S. F. R. Khadri, K. V. Subbarao, and T. Thodarson (2009), Determination of rapid Deccan eruptions across the Cretaceous-Tertiary boundary using paleomagnetic secular variation: 2. Constraints from analysis of eight new sections and synthesis for a 3500-m-thick composite section, *J. Geophys. Res.*, *114*, B06103, doi:10.1029/2008JB005644.

Christensen, U. R., J. Aubert, and G. Hulot (2010), Conditions for Earth-like geodynamo models, *Earth Planet. Sci. Lett.*, *296*(3–4), 487–496, doi:10.1016/j.epsl.2010.06.009.

Clement, B. M. (1991), Geographical distribution of transitional VGPs: Evidence for non-zonal equatorial symmetry during the Matuyama-Brunhes geomagnetic reversal, *Earth Planet. Sci. Lett.*, *104*(1), 48–58, doi:10.1016/0012-821X(91)90236-B.

Clement, B. M. (2004), Dependence of the duration of geomagnetic polarity reversals on site latitude, *Nature*, *428*, 637–640, doi:10.1038/nature02459.

Clement, B. M., D. V. Kent, and N. D. Opdyke (1982), Brunhes-Matuyama polarity transition in three deep-sea sediment cores, *Philos. Trans. R. Soc. London*, *306*, 113–119, doi:10.1098/rsta.1982.0071.

Coe, R. S., L. Hongre, and G. A. Glatzmaier (2000), An examination of simulated geomagnetic reversals from a palaeomagnetic perspective, *Philos. Trans. R. Soc. London*, *358*(1768), 1141–1170, doi:10.1098/rsta.2000.0578.

Coe, R. S., B. S. Singer, M. S. Pringle, and X. Zhao (2004), Matuyama-Brunhes reversal and Kamikatsura event at Maui: Paleomagnetic directions, $^{40}Ar/^{39}Ar$ ages and implications, *Earth Planet. Sci. Lett.*, *222*, 667–684, doi:10.1016/j.epsl.2004.03.003.

Cogné, J. P. (2003), PaleoMac: A MacintoshTM application for treating paleomagnetic data and making plate reconstructions, *Geochem. Geophys. Geosyst.*, *4*(1), 1007, doi:10.1029/2001GC000227.

Dagley, P., and E. Lawley (1974), Paleomagnetic evidence for the transitional behaviour of the geomagnetic field, *Geophys. J. R. Astron. Soc.*, *36*, 577–598, doi:10.1111/j.1365-246X.1974.tb00614.x.

Fuller, M., L. Williams, and K. A. Hoffman (1979), Paleomagnetic records of geomagnetic field reversals and the morphology of the transitional fields, *Rev. Geophys.*, *17*, 179–203, doi:10.1029/RG017i002p00179.

Gallet, Y., A. S. Genevey, and V. Courtillot (2003), On the possible occurrence of 'archaeomagnetic jerks' in the geomagnetic field over the past three millennia, *Earth Planet. Sci. Lett.*, *214*(1–2), 237–242, doi:10.1016/S0012-821X(03)00362-5.

Hargraves, R. B., J. Rehacek, and P. R. Hooper (1997), Palaeomagnetism of the Karoo igneous rocks in southern Africa, *S. Afr. J. Geol.*, *100*(3), 195–212.

Herrero-Bervera, E., and J. P. Valet (1999), Paleosecular variation during sequential geomagnetic reversals from Hawaii, *Earth Planet. Sci. Lett.*, *171*(1), 139–148, doi:10.1016/S0012-821X(99)00145-4.

Herrero-Bervera, E., and J. P. Valet (2005), Absolute paleointensity from the Waianae volcanics (Oahu, Hawaii) between the Gilbert-Gauss and the upper Mammoth reversals, *Earth Planet. Sci. Lett.*, *234*, 279–296.

Herrero-Bervera, E., and J. P. Valet (2009), Testing determinations of absolute paleointensity from the 1955 and 1960 Hawaiian flows, *Earth Planet. Sci. Lett.*, *287*(3–4), 420–433, doi:10.1016/j.epsl.2009.08.035.

Herrero-Bervera, E., G. P. L. Walker, G. G. A. Harrison, J. G. Garcia, and L. Kristjansson (1999), Detailed paleomagnetic study of two volcanic polarity transitions recorded in eastern Iceland, *Phys. Earth Planet. Inter.*, *115*(2), 119–135.

Heunemann, C., D. Krasa, H. C. Soffel, E. Gurevitch, and V. Bachtadse (2004), Directions and intensities of the Earth's magnetic field during a reversal: Results from the Permo-Triassic Siberian trap basalts, Russia, *Earth Planet. Sci. Lett.*, *218*(1–2), 197–213, doi:10.1016/S0012-821X(03)00642-3.

Hillhouse, J., and A. Cox (1976), Brunhes-Matuyama polarity transition, *Earth Planet. Sci. Lett.*, *29*, 51–64, doi:10.1016/0012-821X(76)90025-X.

Hoffman, K. A. (1977), Polarity transition records end the geomagnetic dynamo, *Science*, *196*, 1329–1332, doi:10.1126/science.196.4296.1329.

Hoffman, K. A. (1992), Dipolar reversal states of the geomagnetic field and core-mantle dynamics, *Nature*, *359*(6398), 789–794, doi:10.1038/359789a0.

Hoffman, K. A., and B. S. Singer (2008), Magnetic source separation in Earth's outer core, *Science*, *321*(5897), 1800, doi:10.1126/science.1159777.

Hongre, L., G. Hulot, and A. Khokhlov (1998), An analysis of the geomagnetic field over the past 2000 years, *Phys. Earth Planet. Inter.*, *106*(3–4), 311–335, doi:10.1016/S0031-9201(97)00115-5.

Jarboe, N. A., R. S. Coe, P. R. Renne, J. M. G. Glen, and E. A. Mankinen (2008), Quickly erupted volcanic sections of the Steens Basalt, Columbia River Basalt Group: Secular variation, tectonic rotation, and the Steens Mountain reversal, *Geochem. Geophys. Geosyst.*, *9*, Q11010, doi:10.1029/2008GC002067.

Jourdan, F., G. Féraud, H. Bertrand, M. K. Watkeys, and P. R. Renne (2008), The $^{40}Ar/^{39}Ar$ ages of the sill complex of the Karoo large igneous province: Implications for the Pliensbachian-Toarcian climate change, *Geochem. Geophys. Geosyst.*, *9*, Q06009, doi:10.1029/2008GC001994.

Knight, K. B., S. Nomade, P. R. Renne, A. Marzoli, H. Bertrand, and N. Youbi (2004), The Central Atlantic Magmatic Province at the Triassic-Jurassic boundary: Paleomagnetic and $^{40}Ar/^{39}Ar$ evidence from Morocco for brief, episodic volcanism, *Earth Planet. Sci. Lett.*, *228*(1–2), 143–160, doi:10.1016/j.epsl.2004.09.022.

Kosterov, A. A., and M. Perrin (1996), Paleomagnetism of the Lesotho basalt, southern Africa, *Earth Planet. Sci. Lett.*, *139*(1–2), 63–78, doi:10.1016/0012-821X(96)00005-2.

Laj, C., A. Mazaud, R. Weeks, M. Fuller, and E. Herrero-Bervera (1991), Geomagnetic reversal paths, *Nature*, *351*(6326), 447, doi:10.1038/351447a0.

Langereis, G. C., A. A. M. Van Hoof, and P. Rochette (1992), Longitudinal confinement of geomagnetic reversal paths as a possible sedimentary artefact, *Nature*, *358*, 226–230, doi:10.1038/358226a0.

Leonhardt, R., and K. Fabian (2007), Paleomagnetic reconstruction of the global geomagnetic field evolution during the Matuyama/Brunhes transition: Iterative Bayesian inversion and independent verification, *Earth Planet. Sci. Lett.*, *253*(1–2), 172–195, doi:10.1016/j.epsl.2006.10.025.

Love, J. J. (1998), Paleomagnetic volcanic data and geometric regularity of reversals and excursions, *J. Geophys. Res.*, *103*, 12,435–12,452, doi:10.1029/97JB03745.

Mankinen, E. A., M. Prévot, C. S. Grommé, and R. S. Coe (1985), The Steens mountain (Oregon) geomagnetic polarity transition: 1. Directional variation, duration of episodes, and rock magnetism, *J. Geophys. Res.*, *90*, 10,393–10,416, doi:10.1029/JB090iB12p10393.

Marsh, J. S., and H. V. Eales (1984), The chemistry and petrogenesis of igneous rocks of the Karoo central area, southern Africa, in *Petrogenesis of the Volcanic Rocks of the Karoo Province*, edited by A. J. Erlank, *Spec. Publ. Geol. Soc. S. Afr.*, *13*, 27–68.

McElhinny, M. W., and R. T. Merrill (1975), Geomagnetic secular variation over the past 5 m.y., *Rev. Geophys.*, *13*, 687–708, doi:10.1029/RG013i005p00687.

McFadden, P. L., and W. McElhinny (1988), The combined analysis of remagnetization circles and direct observations in palaeomagnetism, *Earth Planet. Sci. Lett.*, *87*(1–2), 161–172, doi:10.1016/0012-821X(88)90072-6.

McFadden, P. L., and M. W. McElhinny (1990), Classification of the reversal test in paleomagnetism, *Geophys. J. Int.*, *103*, 725–729, doi:10.1111/j.1365-246X.1990.tb05683.x.

Moulin, M. (2011), Les traps du Karoo et les extinctions du Jurassique inférieur: Dynamique éruptive et perturbations de l'environnement, M.S. thesis, 305 pp., Inst. de Phys. du Globe de Paris, Paris.

Moulin, M., F. Fluteau, V. Courtillot, J. Marsh, G. Delpech, X. Quidelleur, M. Gérard, and A. E. Jay (2011), An attempt to constrain the age, duration, and eruptive history of the Karoo flood basalt: Naude's Nek section (South Africa), *J. Geophys. Res.*, *116*, B07403, doi:10.1029/2011JB008210.

Olson, P. L., G. A. Glatzmaier, and R. S. Coe (2011), Complex polarity reversals in a geodynamo model, *Earth Planet. Sci. Lett.*, *304*, 168–179.

Pavlov, V., F. Fluteau, R. Veselovsky, and A. Fetisova (2010), Geomagnetic secular variations and volcanic pulses in the Siberian traps, *Geophys. Res. Abstr.*, *12*, 5872.

Prévot, M., and P. Camps (1993), Absence of preferred longitude sectors for poles from volcanic records of geomagnetic reversals, *Nature*, *366*(6450), 53–57, doi:10.1038/366053a0.

Prévot, M., E. A. Mankinen, C. S. Grommé, and R. S. Coe (1985), Absence of longitudinal confinement of poles in volcanic records of geomagnetic reversals, *Nature*, *316*, 230–234.

Prévot, M., N. Roberts, J. Thompson, L. Faynot, M. Perrin, and P. Camps (2003), Revisiting the Jurassic geomagnetic reversal recorded in the Lesotho Basalt (southern Africa),

Geophys. J. Int., *155*, 367–378, doi:10.1046/j.1365-246X.2003.02029.x.

Quidelleur, X., and J. P. Valet (1994), Paleomagnetic records of excursions and reversals: Possible biases caused by magnetization artefacts?, *Phys. Earth Planet. Inter.*, *82*, 27–48, doi:10.1016/0031-9201(94)90100-7.

Quidelleur, X., and J. P. Valet (1996), Geomagnetic changes across the last reversal recorded in lava flows from LaPalma, Canary islands, *J. Geophys. Res.*, *101*, 13,755–13,773, doi:10.1029/95JB03740.

Quidelleur, X., J. Holt, and J. P. Valet (1995), Confounding influence of magnetic fabric on sedimentary records of a field reversal, *Nature*, *374*, 246–249, doi:10.1038/374246a0.

Riisager, P., and N. Abrahamsen (2000), Paleointensity of West Greenland Palaeocene basalts: Asymmetric intensity around the C27n-C26r transition, *Phys. Earth Planet. Inter.*, *118*(1–2), 53–64, doi:10.1016/S0031-9201(99)00125-9.

Riisager, P., J. Riisager, N. Abrahamsen, and R. Waagstein (2002), New paleomagnetic pole and magnetostratigraphy of Faroe Islands flood volcanics, North Atlantic igneous province, *Earth Planet. Sci. Lett.*, *201*(2), 261–276, doi:10.1016/S0012-821X(02)00720-3.

Riisager, J., P. Riisager, and A. K. Pedersen (2003), Paleomagnetism of large igneous provinces: Case-study from West Greenland, North Atlantic igneous province, *Earth Planet. Sci. Lett.*, *214*(3–4), 409–425, doi:10.1016/S0012-821X(03)00367-4.

Rochette, P. (1990), Rationale of geomagnetic reversal versus remanence recording process in rocks: A critical review, *Earth Planet. Sci. Lett.*, *98*, 33–39, doi:10.1016/0012-821X(90)90086-D.

Valet, J. P., and E. Herrero-Bervera (2003), Some characteristics of geomagnetic reversals inferred from detailed volcanic records, *C. R. Geosci.*, *335*(1), 79–90, doi:10.1016/S1631-0713(03)00005-1.

Valet, J. P., and E. Herrero-Bervera (2011), A few characteristic features of the geomagnetic field during reversals, in *The Earth's Magnetic Interior*, edited by E. Petrovsky, D. Ivers, and T. Harinarayana, pp. 139–151, Springer, Netherlands, doi:10.1007/978-94-007-0323-0_10.

Valet, J. P., and C. Laj (1984), Invariant and changing transitional field configurations in a sequence of geomagnetic reversals, *Nature*, *311*(5986), 552–555, doi:10.1038/311552a0.

Valet, J. P., and G. Plenier (2008), Simulations of a time-varying non-dipole field during geomagnetic reversals and excursions, *Phys. Earth Planet. Inter.*, *169*(1–4), 178–193, doi:10.1016/j.pepi.2008.07.031.

Valet, J. P., C. Laj, and C. G. Langereis (1988), Sequential geomagnetic reversals recorded in upper tortonian marine clays in western Crete (Greece), *J. Geophys. Res.*, *93*(B2), 1131–1151, doi:10.1029/JB093iB02p01131.

Valet, J. P., L. Tauxe, and B. M. Clement (1989), Equatorial and mid-latitudes records of the last geomagnetic reversal from the Atlantic Ocean, *Earth Planet. Sci. Lett.*, *94*, 371–384, doi:10.1016/0012-821X(89)90154-4.

Valet, J. P., P. Tucholka, V. Courtillot, and L. Meynadier (1992), Palaeomagnetic constraints on the geometry of the geomagnetic field during reversals, *Nature*, *356*(6368), 400–407, doi:10.1038/356400a0.

van Zijl, J. S. V., K. W. T. Graham, and A. L. Hales (1962a), The palaeomagnetism of the Stormberg lavas of South Africa 1: Evidence for a genuine reversal of the Earth's field in Triassic–Jurassic times, *Geophys. J. R. Astron. Soc.*, *7*, 23–39, doi:10.1111/j.1365-246X.1962.tb02250.x.

van Zijl, J. S. V., K. W. T. Graham, and A. L. Hales (1962b), The palaeomagnetism of the Stormberg lavas of South Africa 2: The behaviour of the magnetic field during a reversal, *Geophys. J. R. Astron. Soc.*, *7*, 169–182, doi:10.1111/j.1365-246X.1962.tb00366.x.